Marine Research/ DOI:10.29677/ MR.202206_2(1).0003

Numerical Simulation of Dynamic Cable Used For Floating Offshore Substation

Yu-Chi Hung [1] Hung-Jie Tang [2] Chuan-Tsang Lee [3]
Wai Wa Ng [1] Ray-Yeng Yang [1*]

[1] *Department of Hydraulic and Ocean Engineering, National Cheng Kung University, Taiwan*
[2] *Tainan Hydraulics Laboratory, National Cheng Kung University, Taiwan*
[3] *National Academy of Marine Research, Taiwan*

ABSTRACT

In this study, an area of relatively shallow waters (about 50 meters to 100 meters of water depth) was selected for the designing of a floating substation, and a barge type platform was used to provide sufficient space on the platform for the substation main body space configuration. A catenary mooring system was used to restrict the movement of the platform to a range, in order to avoid random drifting exposing nearby marine structures and navigation channels to danger. In terms of power transmission, the research is aimed at finding the tension and curvature of the dynamic cable under extreme sea conditions in Taiwan. Dynamic cable under different water depths, different cable buoy configurations, and different directions will be observed.

After numerical calculations, it is found that the 100-meter deep dynamic cable configuration is more appropriate for installation than the 50-meter deep dynamic cable configuration. As there is more space for the cable to be compressed or stretched, the improved dynamic cable can be applied to the water depth of 100 meters in this research. With the water depth of 50 meters, the dynamic cable can be placed closer to the seabed or to configure cable in a double wave shape, so that the space for cable movement can be increased horizontally. However, even with the improved configuration, only the downstream direction cables of case 2 and case 3are maintainable.

Moreover, the failure location of dynamic cable is different under configurations with different angles. With the 0-degree configuration, the touchdown point of dynamic cable is prone to torsional deflection, which causes excessive curvature. With the 90-degree configuration, dynamic cable on the seabed is displaced with a large range. Under the 180-degree configuration, the S-shaped curve configuration of dynamic cable disappears, which causes the tension to increase. These phenomena can be used as a reference and improvement direction for dynamic cable design in the future.

Keywords: floating substation, dynamic cable design, mooring cable design, tension force, curvature.

* Corresponding author, E-mail: ryyang@mail.ncku.edu.tw

Received 1 March 2022, Accepted 29 April 2022.

1 INTRODUCTION

With the development of floating wind turbines in recent years, a large number of floating wind turbines will be deployed in offshore wind farms in the future. After electricity is generated, the power must be collected and transported for use in domestic or industrial use. Therefore, floating substations and dynamic cables will be key components for offshore wind farms. If the power generated by offshore wind turbines is directly transferred via cables, a large amount of power will be consumed during transmission. Therefore, it is necessary to collect the power from the offshore substation in order to boost and transfer it to land, which can avoid the issue of power loss. Therefore, floating substations design concepts have emerged, such as substations in the US (Shelley et al., 2020), the Fukushima Project, IDEOL (Alexandre et al., 2018), etc. In addition, the number of cables going ashore will be reduced with the construction of offshore substations. As the promotion of the offshore wind power industry in Taiwan is continuing, there is a need of research on offshore substations.

Since there are few actual cases of floating substations, a barge-type floating substation has been designed independently for this study. The catenary mooring is used as the mooring system, with different dynamic cable configurations mounted below.

The purpose of this research is to conduct numerical simulations for different cable configurations to explore the changes in tension and curvature of each set of dynamic cables under normal and extreme environmental conditions in Taiwan.

2 RESEARCH METHOD

2.1 Numerical software

2.1.1 Hydrodynamic theory and calculation

The professional hydrodynamic analysis software AQWA is used for hydrodynamic calculation. AQWA is usually used for studying the impact of environmental loads such as wind, wave, and current, on fixed and floating structures. The boundary element method is used as it is appropriate to solve the effects of First- and Second-order wave force in both time domain and frequency domain.

With AQWA, potential flow theory and diffraction theory are used to calculate hydrodynamic issues, including added mass, radiation damping, first-order wave force, second-order wave force and hydrostatic stiffness. The force of wave field is divided into 2 categories: wave force and dynamic response of the floating platform. There are two kinds of wave force, including first- and second-order wave force. First-order wave force includes incident wave force such as wave frequency in terms of Froude-Krylov force and diffraction and radiation force caused by the existence of an object. In addition, second-order wave force mainly includes the wave drift force. If the frequency is similar to the natural frequency of the object, the object tends to drift slowly. QTF (Quadratic Transfer Function, QTF) describes the relationship between a wave force expressed by the surface elevation and the resulting slow drift force. QTF calculation is used in AQWA to calculate the second-wave force.

2.1.2 Time domain analysis

In this study, OrcaFlex is used for numerical simulation of time-domain. OrcaFlex is widely used in evaluating the stability of offshore floating structures and designing anchoring systems, such as ships and floating wind turbines, etc. The equation for calculating time-domain of floating platforms in OrcaFlex is as follows,

$$M(p,a) + C(p,v) + K(p) = F(p,v,t) \quad (1)$$

where $M(p,a)$ = inertial force of platform,

$C(p,v)$ = damping force of platform,

$K(p)$ = stiffness force of platform

$F(p, v, t)$ = external force,

p, v, a, t = position, velocity vector, acceleration vector and simulation time respectively.

Implicit time domain integration is provided in OrcaFlex to solve equations of motion. In the numerical simulation, Chung and Hulbert's generalized–a integration scheme is used. At the beginning of numerical simulation, the force and torque of each object are all simulated, including weight, buoyancy, drag of hydrodynamic and aerodynamic force, effect of hydrodynamic added mass, tension and shear force, seabed friction, bending and torque and contact forces with objects, etc. Equations of motion are solved at the end of the given time step. Since p, v, a are unknown, the iterative method is required in this case.

Morison's equation is used in OrcaFlex for the calculation of the hydrodynamic forces of mooring lines, power cables, etc. The lumped mass method is used in OrcaFlex to solve the motion of the mooring lines and power cables. Morison's equation is used to calculate the wave loads on fixed cylinders, including inertial forces related to fluid acceleration, and drag related to fluid velocity,

$$f = C_m \Delta a_f + \frac{1}{2} \rho C_d A |v_f| v_f \tag{2}$$

where f = wave load on the structure,

C_m= the inertia coefficient of the structure,

Δ = the drainage volume of the structure,

a_f= the acceleration of the fluid relative to the earth,

ρ = fluid density,

C_d= the resistance coefficient of the structure,

A = the area of the structure subject to fluid resistance,

v_f=the velocity of the fluid relative to the earth.

2.2 Floating substation design

Considering Taiwan's current ocean engineering energy, the semi-submersible platform has good mobility and does not require unique installation vessels. Among them, the construction of the barge-type platform is relatively simple, so this study uses a barge-type floating platform, which is appropriate for the substation facilities construction in the future.

IDEOL has developed a foundation based on a patented damping pool (Alexandre et al., 2018). Chuang et al. (2021) referred to the moon pool concept in IDEOL's Barge-type floating platform to design a barge-type platform that conforms to Taiwan waters. Moreover, it has stable motion changes in numerical simulation and physical experiments, and the draft is also suitable for the site of this study, so it is selected as the platform for carrying the substation.

According to the substation specification from Lai, Z. N. (2018), a substation with a capacity of 100-150MW is assumed to be 30m×30m×20m in length, width and height, respectively, and the substation weight is about 1,000 tons. A schematic diagram of floating substation and detailed parameters is as shown in Figure 1.

In Taiwan, the offshore wind farm is planned to be installed at the water depth of 50 meters to 100 meters, so water depths of 50 meters and 100 meters will be used for design in this study.

In this study, the mooring design is based on catenary theory. By adjusting the various mooring diameters, the mooring wet weight and horizontal distance between floater and anchor, two different floating deep-water mooring substations can be drawn. The parameters for 50-meter and 100-meter water depth mooring systems are given in Table 1 below.

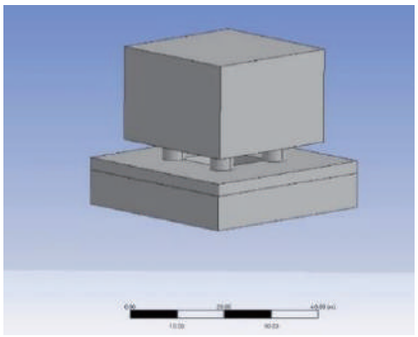

Barge-type floating platform size	40 m*40 m*10 m
Substation size	30 m*30 m*20 m
Total weight (including substation and platform)	10,540 ton
Draught	7.4 m
Center of gravity	(0 m, 0 m, 5.4 m)

Figure 1. Floating substation parameters.

Table 1. Mooring cable parameter (50 and 100-meter water depths).

Water depth	50 meters	100 meters
Number of moorings	4*2	4*2
Angle between the mooring line and wave incidence	30˚, 45˚	30˚, 45˚
Mooring length	400 m	400 m
Horizontal projection distance between anchor point and fairlead	376 m	376 m
Mooring diameter	0.15 m	0.15 m
Weight per unit length of mooring	447.75 kg/m	447.75 kg/m
Mooring material grade	R4	R4
Minimum breaking load (MBL)	19,730 kN	19,730 kN
Mooring configurations	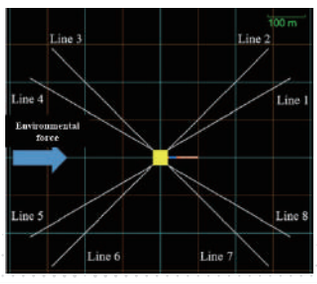	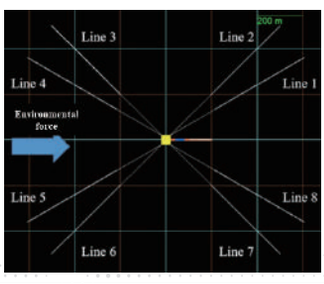

2.3 Dynamic cable design and configuration

The dynamic cable used in this research is according to the 66kV dynamic cable provided by Manuel UT Rentschler et al. (2020). The basic parameters of the cable are as Table 2 shown. Manuel U. T. Rentschler et al. (2019) stated the configuration of dynamic cable under static state. The total length of cable would be 2.8 times the distance of bottom of platform to seabed. The cable section with buoys is started from the junction of platform, and the length is a quarter of the total length of cable.

The purpose of this study is to investigate the changes in tension and curvature of the dynamic cable with different water depths. Therefore, the optimal configuration with the static state is set as case 1. In case 2, the position of buoyancy module is changed to confirm it is in the middle of the cable. In case 3, the double wave shape cable configuration will be used for simulation according to Zhao et al. (2021). In order to obtain a common comparison value, the design of a catenary mooring system is used as a basis for comparison with other dynamic cable schemes. Dynamic cables are located on the downstream direction (0 degrees), lateral direction (90 degrees) and upstream direction (180 degrees) according to their placement positions. The different scheme configurations and placement positions are as Table 3 to Table 4 as well as Figure 2 to Figure 4 shown.

In this study, the fitness parameters proposed in Manuel UT Rentschler et al. (2019) are used to discuss the feasibility of different configuration of cables. The definition of the fitness parameter is shown in formula 1. The fitness parameter is composed of the addition of two sets of ratios, which are the ratio of the maximum tension (T_{max}) in time series to the minimum breaking load (MBL) and the ratio of the maximum curvature (ρ_{max}) in time series to the maximum allowable curvature (MAC).

$$Fitness = \frac{T_{max}}{MBL} + \frac{\rho_{max}}{MAC} \tag{3}$$

Table 2. Basic parameters of dynamic cable.

Dynamic cable	Diameter	200 mm
	Unit weight in water	390 N/m
	Bending stiffness	10 kNm^2
	Axial stiffness	700 MN
	Minimum breaking load	100 kN
	Minimum bending radius	2 m
Buoyancy section	Diameter	306 mm
	Net buoyancy	316 N/m

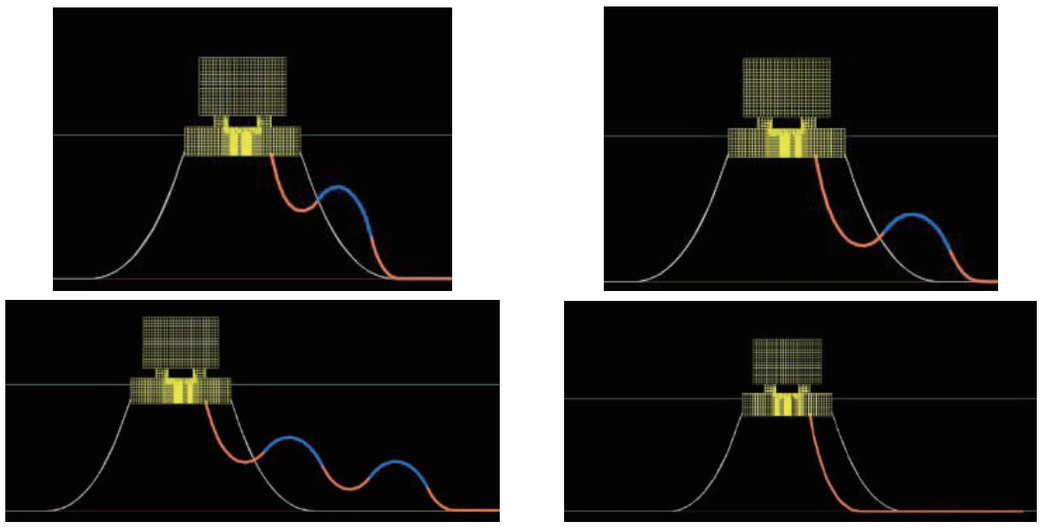

Figure 2. Dynamic cable layout (50 meters water depth) (Upper left: case 1, upper right: case 2, lower left: case 3, lower right: catenary type).

Table 3. Dynamic cable configuration parameter (50 meters water depth).

	Case 1	Case 2	Case 3	Catenary type
Cable total length	124 m	124 m	195 m	124 m
Projection distance	88 m	88 m	155 m	88 m
Length of section with buoyancy modules	31 m	31 m	30 m, 30 m	No floating section
Starting position of buoyancy modules	31 m	46.5 m	40 m, 95 m	No floating section

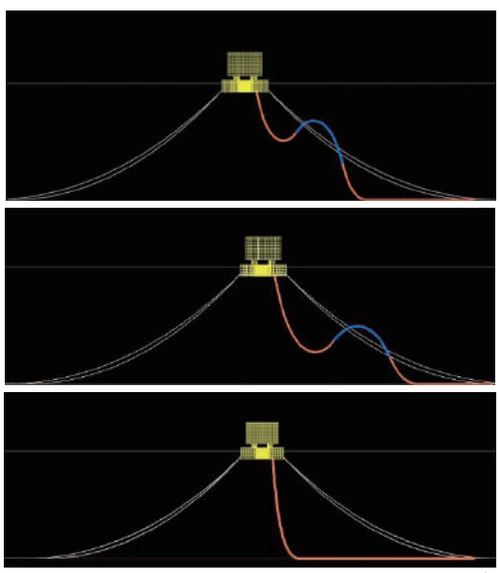

Figure 3. Dynamic cable layout (100-meter water depth) (Upper: case 1, middle: case 2, bottom: catenary type).

Table 4. Dynamic cable configuration parameter (100-meter water depth).

	Case 1	Case 2	Catenary type
Cable total length	264 m	264 m	264 m
Projection distance	188 m	188 m	188 m
Length of section with buoyancy modules	66 m	66 m	No float section
Starting position of buoyancy modules	66 m	99 m	No float section

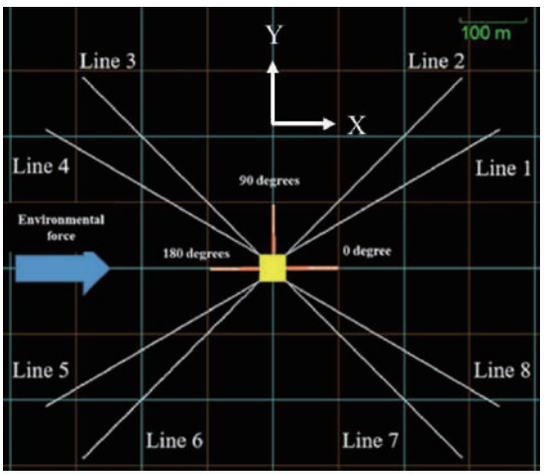

Figure 4. Schematic diagram of dynamic cable angle configuration.

2.4 Environmental condition selection

According to Chao and Young (2006) and "Demonstration Incentives for Offshore Wind Power" (2019), four kinds of simulation conditions of Hsinchu area can be obtained. The total length of simulation time is 7,200 s, and three external forces are in the same direction. Table 5 illustrates different conditions.

Table 5. Comparison table of simulation conditions.

	Wave conditions	Current conditions	Wind speed conditions
Normal sea condition	JONSWAP (γ=2.08) Significant wave height (H1/3) 0.97 m, Peak period (Tp) 4.1 s	0.5 m/s	6.8 m/s
Northeast monsoon sea condition	JONSWAP (γ=2.08) Significant wave height (H1/3) 1.3 m, Peak period (Tp) 4.8 s	0.5 m/s	17.1 m/s

	Wave conditions	Current conditions	Wind speed conditions
10-year return period condition	JONSWAP (γ=2.08) Significant wave height (H1/3) 9 m, Peak period (Tp) 12 s	1 m/s	37.2 m/s
50-year return period condition	JONSWAP (γ=2.08) Significant wave height (H1/3) 11.8 m, Peak period (Tp) 13.8 s	1 m/s	41.1 m/s

3 RESULTS AND DISCUSSION

3.1 Mooring design inspection

During the process of designing the catenary mooring line, the following two requirements must be met under the condition of the 50-year return period, namely:

1. The mooring line must touch the ground before the anchor point;
2. The maximum tension of the mooring line does not exceed the minimum breaking load of the mooring line itself.

In this research, the wave conditions of a 50-year typhoon return period will be used for the inspection of mooring design. The mooring systems of 50-meter and 100-meter water depths will be tested with two upstream mooring cables numbered Line 3 and Line 4. Figure 5 and Figure 6 depict that when the two groups of mooring lines are moving on the platform, there is a certain length of mooring lines that lie across on the seabed to avoid vertical upward pull on the anchor points. The fairlead tensions of Line 3 and Line 4 are 6349 kN and 8798 kN, respectively, at the 50-meter depth. The fairlead tensions of Line 3 and Line 4 are 5700 kN and 5225 kN, respectively, at the 100-meter depth. All the tensions of mooring lines are less than the minimum breaking load (19,730 kN) of the mooring line, which satisfies relevant inspection conditions.

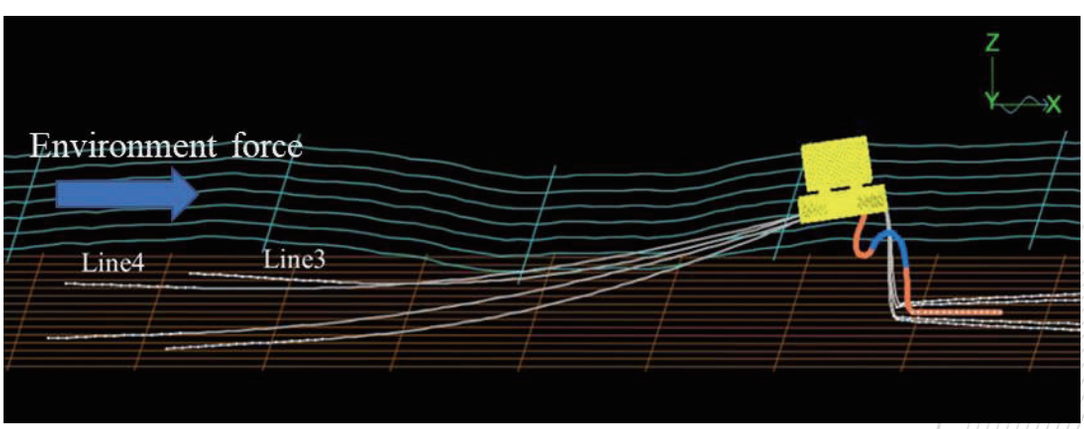

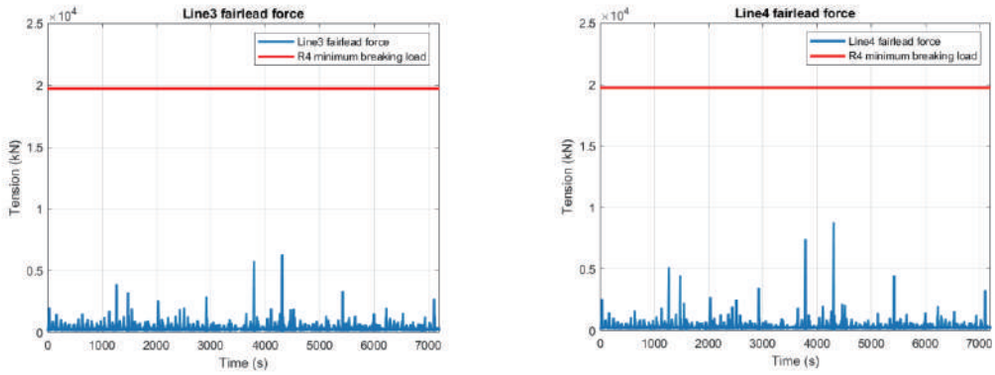

Figure 5. Mooring inspection diagram (50-meter water depth) (Bottom left: Line 3 maximum tension, bottom right: Line 4 maximum tension).

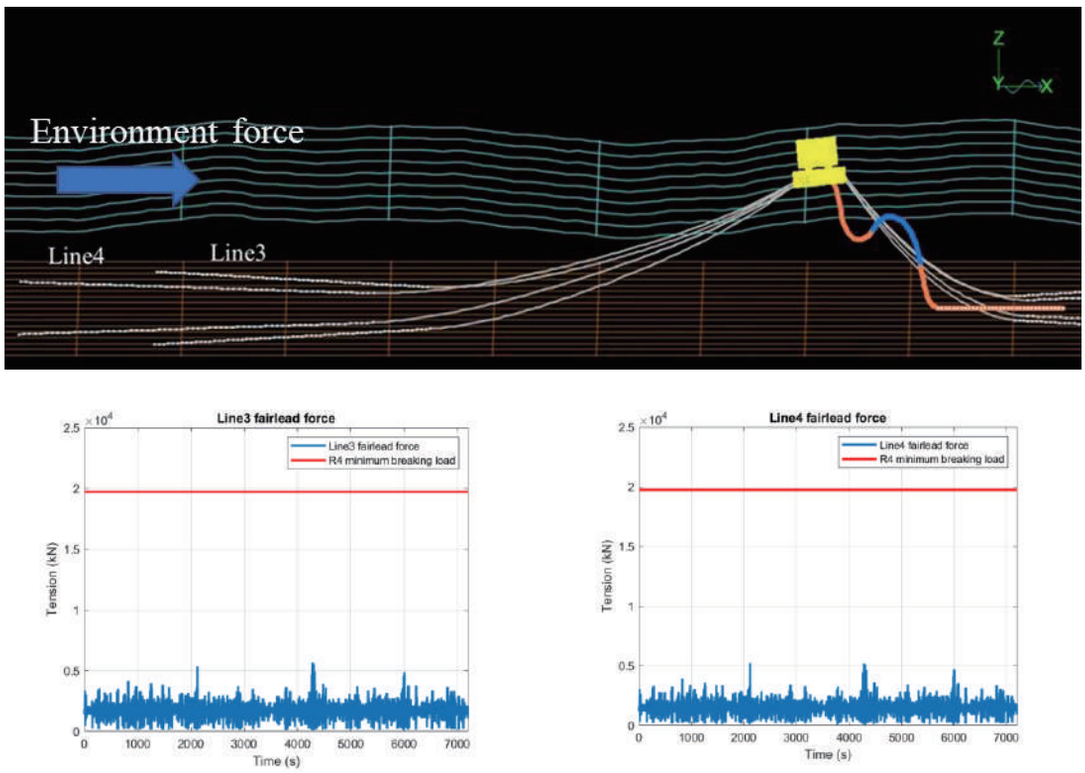

Figure 6. Mooring inspection diagram (100-meter water depth) (Bottom left: Line3 maximum tension, bottom right: Line4 maximum tension).

3.2 Cable simulation results

In this section, the floating substations and cables are simulated using the environmental conditions of Hsinchu, with water depths of 50 meters and 100 meters. Point A represents the sag bend, Point B represents the hog bend section of the cable, and Point C represents the touchdown of the cable, which are shown in Figure 7. Finally, the cable comparison between different schemes and angles is carried out with the fitness parameter.

For the environmental conditions designed in this project, the lower the fitness parameter value, the more suitable the configuration. If the maximum tension of the cable exceeds the minimum breaking load or the maximum curvature of the cable exceeds the maximum allowable curvature, the fitness parameter will be not calculated.

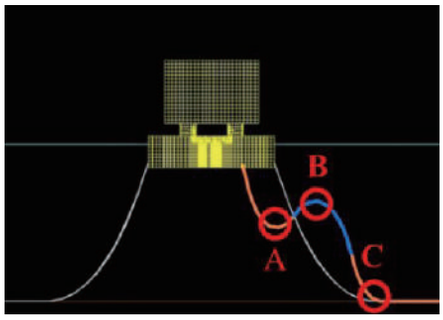

Figure 7. Schematic diagram of tether position code.

3.2.1 The case of 50-meter water depth

First, when the cable is deployed in the downstream direction (0 degrees), the motion of the cable is mainly in a compressed state, and severe distortion will occur at point C of the cable, resulting in a larger curvature value. When the cable is placed in the lateral direction (90 degrees), the cable will be slightly stretched and slightly offset in the ground contact section. In addition, the tension performance may exceed the minimum breaking force of the cable. When the cable is arranged in the upstream direction (180 degrees), the cable mainly bears the tensile force, so the maximum value of the tension part is likely to exceed the minimum breaking force of the cable, and the curvature change is relatively small.

Under the 50-year return period condition, when the catenary type of cable is configured at 90 degrees, the tension and curvature are in line with the material characteristics of the cable itself. The calculated fitness parameter value is 1.29. When the cable is configured at 0 degrees, Point C will be severely twisted and exceed the maximum allowable curvature of the cable. With the 180-degree configuration, the cable is completely straightened, resulting in excessive tension.

There is a cable section with buoyancy modules in case 1. Moreover, the buoyancy modules section is closer to the water surface. In this case, the cable does not have any angle configuration that can meet the characteristics of the material itself. The curvature of the Point C is reduced at 0-degree configuration. However, the tension of the cable tends to rise in the 90-degree configuration, and the cable is completely straightened in the 180-degree configuration, while the tension value exceeds MBL.

The cable section with buoyancy modules in case 2 cable is relatively closer to the seabed, so there is more space for the cable to move. When the cable is configured at 0 degree in this case, the curvature performance of the three points ABC is decreased compared with case 1, but torsion still occurs at point C. The fitness parameter value is 1.2 in this configuration. When the cable is at 90 degrees, the maximum tension exceeds the minimum breaking load of the cable. Under the configuration with 180 degrees, the tension of the cable is not significantly improved.

In case 3, the double wave shape cable is used, which mainly provides more movement space for the cable. Compared with case 2, the curvature performance of the cable C point is lower. When the cable is configured at 0 degrees, the fitness parameter is 1.28. With 90-degree and 180-degree configurations of the cable, the tension exceeds the minimum breaking load of the cable. The tension under the 180-degree condition is significantly reduced, compared with other cases. Figure 11 to Figure 14 are the maximum tension and maximum curvature distribution diagrams of the four cable types. The left column is the maximum tension, and the right column is the maximum curvature. The upper, middle, and lower pictures represent the 0-degree, 90-degree, and 180-degree configurations of the cable, respectively.

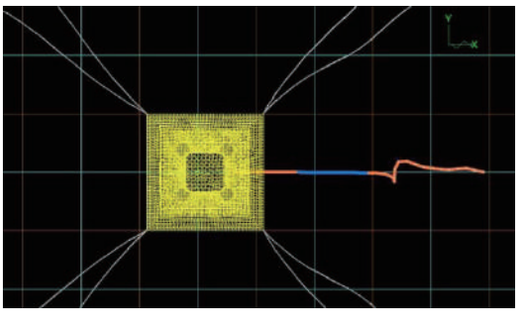

Figure 8. Case 1 cable distortion situation of 0-degree configuration cable.

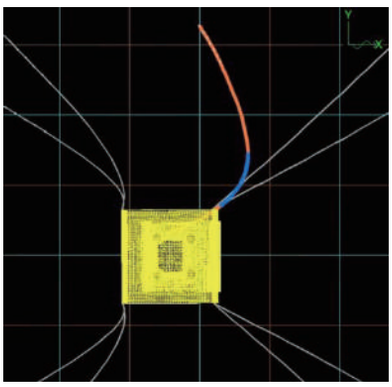

Figure 9. Displacement of the position where the cable is deployed at 90 degrees in case 1.

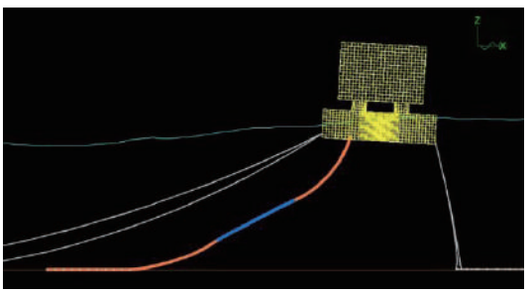

Figure 10. The 180-degree configuration of the cable in case 1.

Table 6. Fitness parameter statistics table (50-meter water depth).

	0 degrees	90 degrees	180 degrees
Catenary type	NAN	1.29	NAN
Case 1	NAN	NAN	NAN
Case 2	1.2	NAN	NAN
Case 3	1.28	NAN	NAN

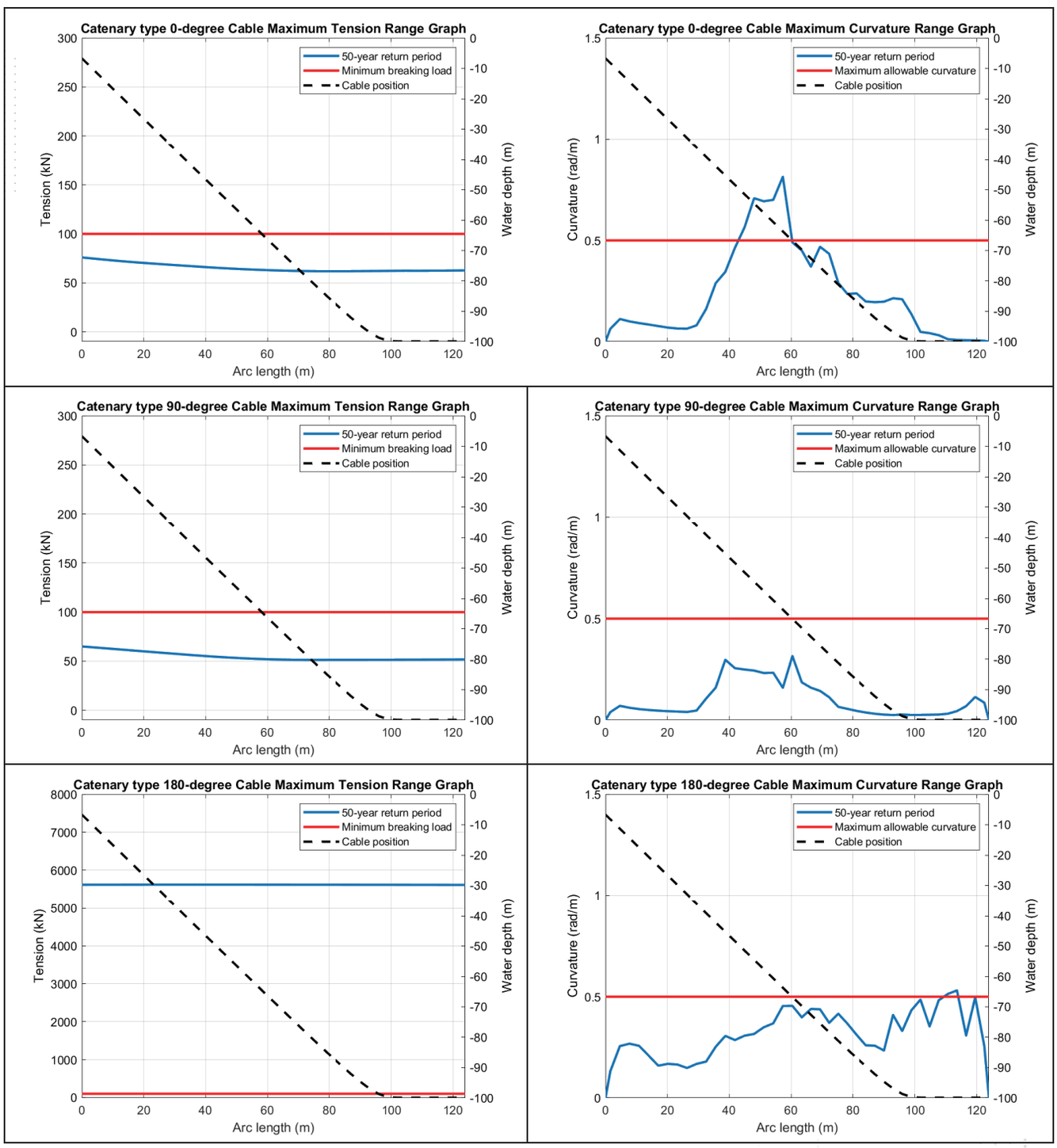

Figure 11. Catenary type cable.

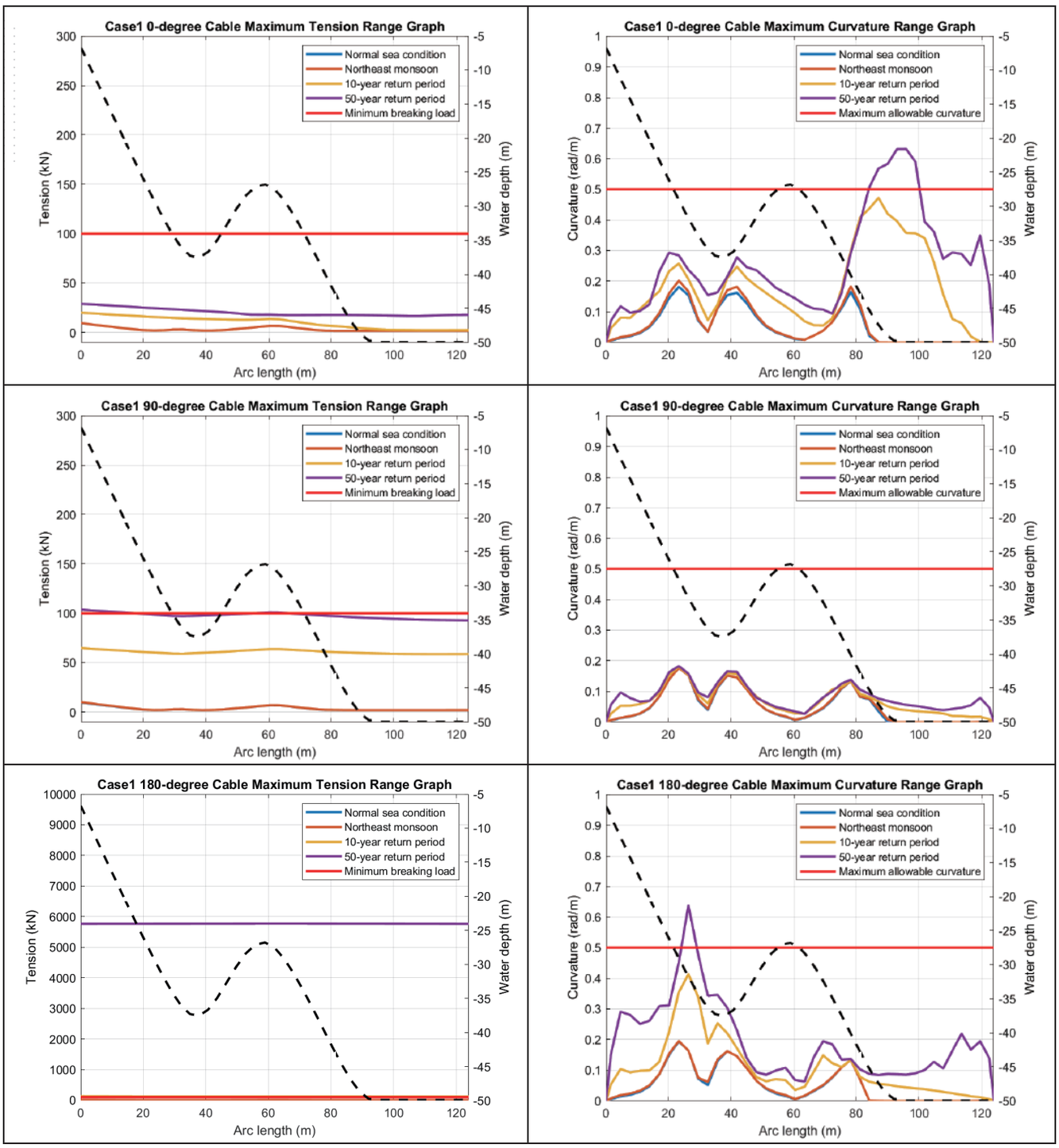

Figure 12. Case 1 dynamic cable.

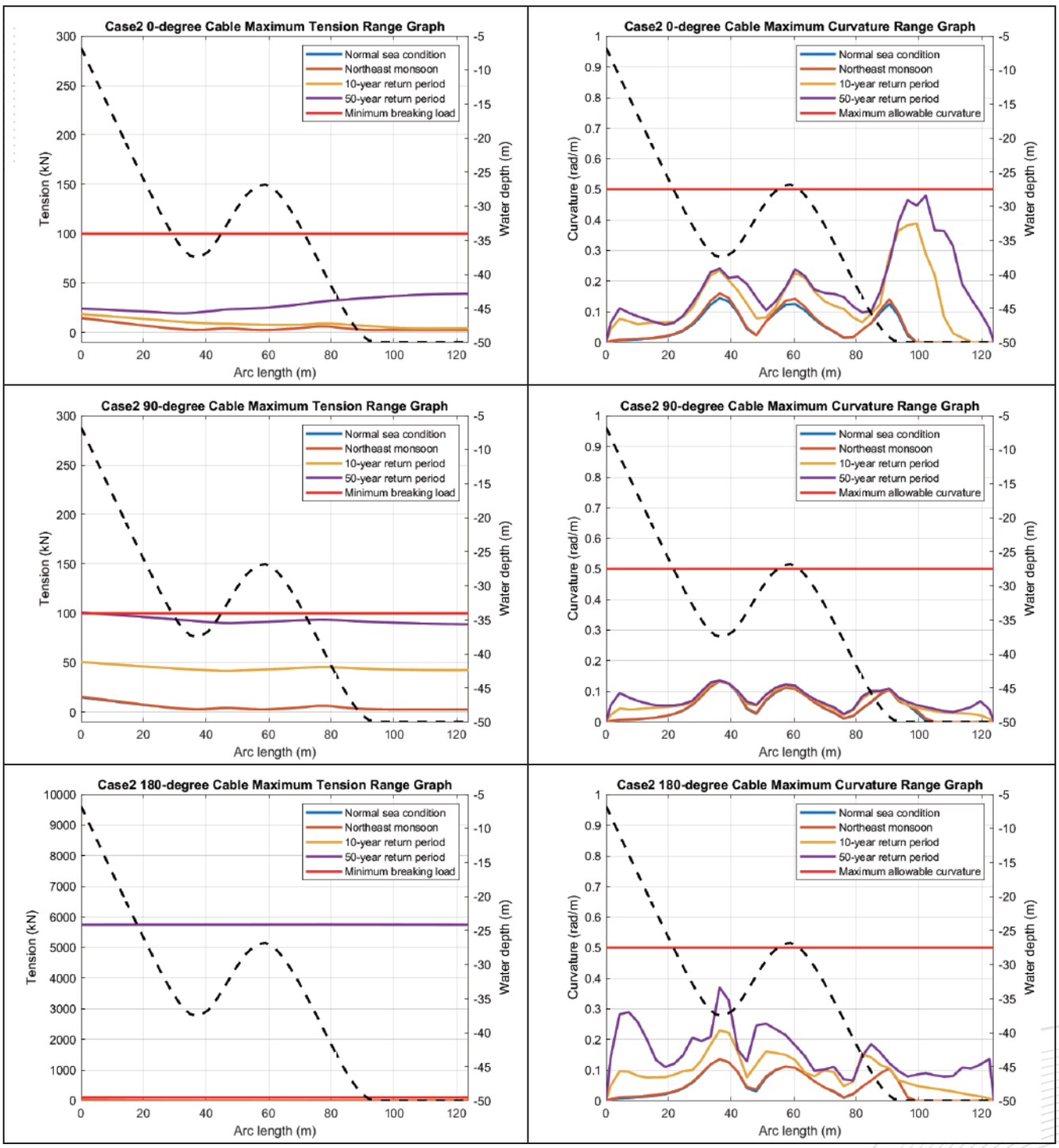

Figure 13. Case 2 dynamic cable.

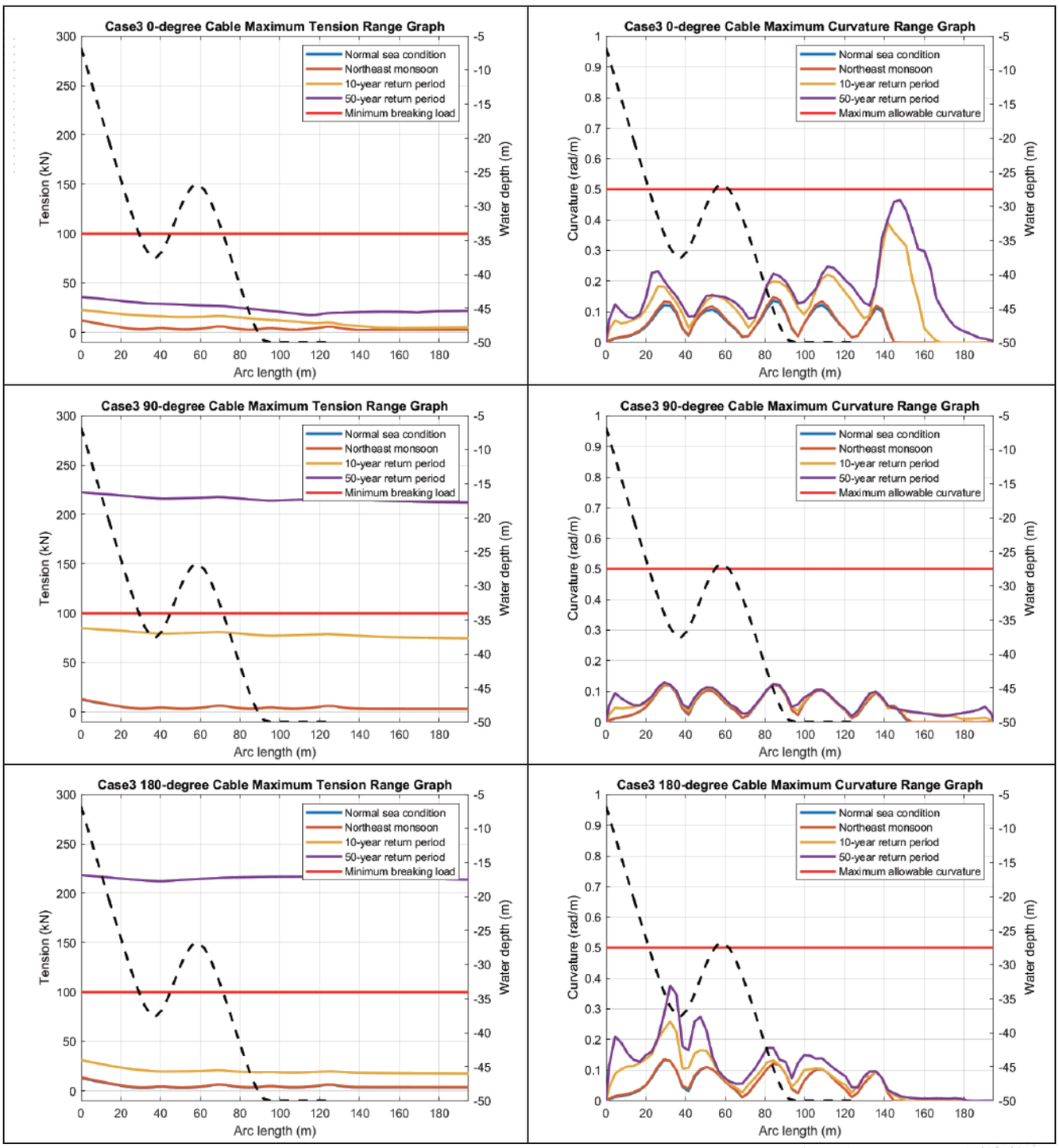

Figure 14. Case 3 dynamic cable.

3.2.2 The case of 100-meter water depth

Compared with the 50-meter water depth, the 100-meter water depth cable configuration provides more space which is enough for movement. Generally, the bending of the cable C point is gentler and the curvature is smaller; but due to the deeper water depth, the initial cable tension value will be larger. There is a little difference between the motion of the cable at three angles and the motion at a water depth of 50 meters.

Under the 50-year return period of the catenary type of cable, only when the 90-degree cable is configured, the tension and curvature can simultaneously meet the material constraints of the cable itself, and its fitness parameter is 1.44. When the cable is configured at 0 degree, the curvature of the cable is too large at point C. While the cable tension value exceeds the minimum breaking load of the cable when configured at 180 degrees.

In case 1, the initial tension and curvature of the catenary type cable are improved with the configuration of the buoyancy module. Therefore, under the conditions of the 50-year regression period, the cable configurations with three different angles meet the restrictions, and their fitness parameters are 1.11, 0.74, and 0.72, respectively. A decrease occurs when it is compared with the case using the catenary cable.

In case 2, the cable section with buoyancy modules is moved closer to the seabed. It is found that the curvatures of the three points ABC of the cable are decreased, but the amplitudes are small. While the tension part of the 180-degree configuration is increased, it is still less than the minimum breaking load. All of the configurations at three angles meet the limits, and the fitness parameters are 0.94, 0.65, and 0.73, respectively. Compared with case 1, the performances at 0 degrees and 90 degrees are better than that of case 1. There is not much difference in the 180-degree configuration. Figure 15 to Figure 17 depict the maximum tension and maximum curvature distribution diagrams of the three configurations of cables. The left column is the maximum tension, and the right column represents the maximum curvature. The upper, middle, and lower pictures represent the 0 degrees, 90 degrees, and 180 degrees configurations of the cable.

Table 7. Fitness parameter statistics table (100-meter water depth).

	0 degrees	90 degrees	180 degrees
Catenary type	NAN	1.44	NAN
Case 1	1.11	0.74	0.72
Case 2	0.94	0.65	0.73

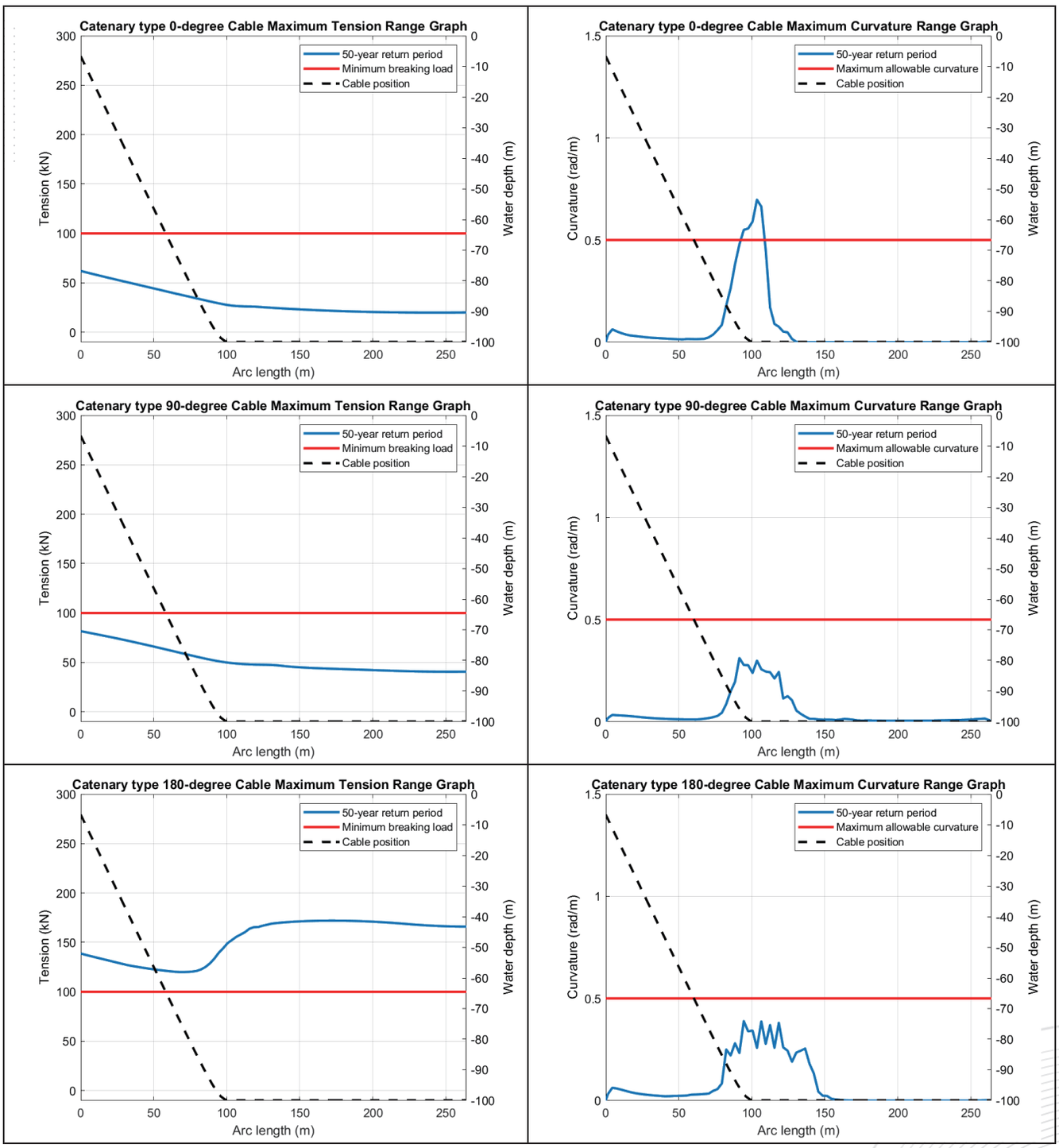

Figure 15. Catenary type cable.

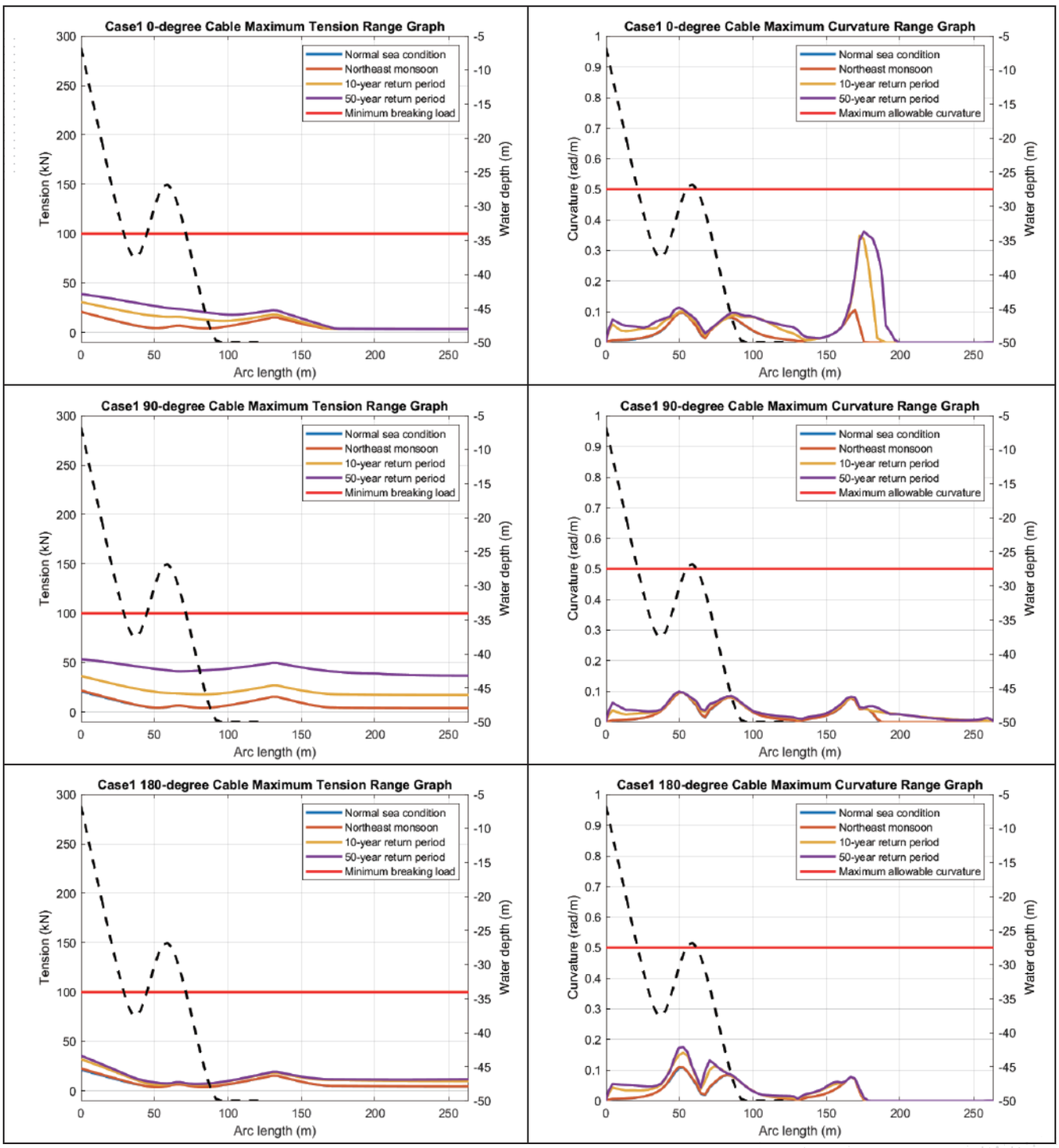

Figure 16. Case 1 dynamic cable.

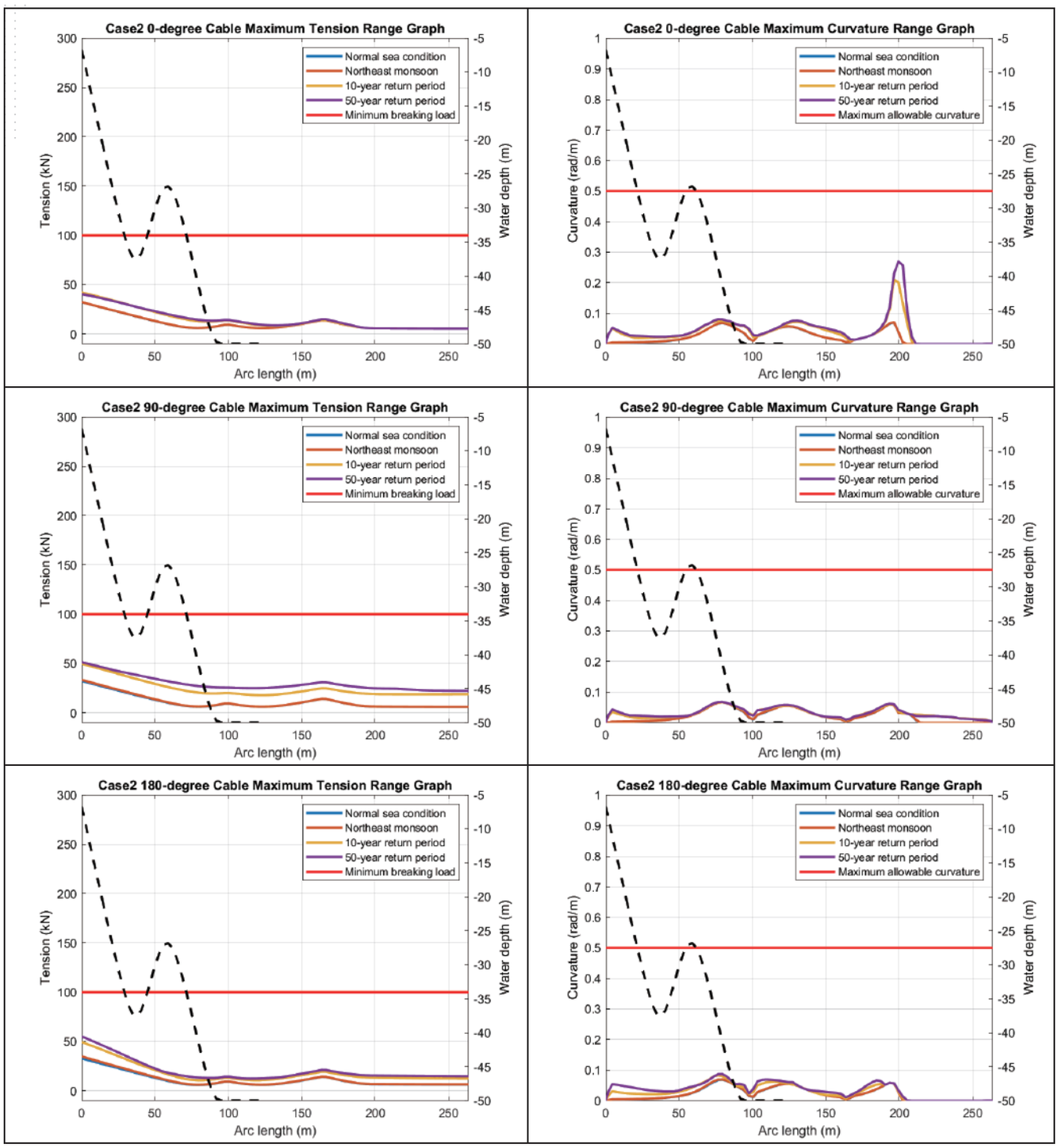

Figure 17. Case 2 dynamic cable.

4 CONCLUSION

Under the condition of Taiwan's 50-year typhoon return period, the cable positions and issues that need to be considered are not the same as those under different angle configurations. In the 0-degree configuration, the cable is affected by the direction of the platform's movement, where compression phenomenon occurs, and the problem of excessive curvature value is likely to occur at the touchdown point of the cable, especially for catenary type of cable. The deep cable buoyancy section configuration (case 2) and double buoyancy module configuration (case 3) can increase the movement space of the cable compression and reduce the curvature of the touchdown point of the cable. Under 0-degree configuration, the cable touchdown point will be offset and twisted, especially in shallow water areas. The twisting state is more obvious, and the cable touchdown point can be optimized in the subsequent design.

In the 90-degree configuration, the cable section suspended in the water often drifts on the downstream side (positive direction of the X-axis), which results in displacement of the cable section on the seabed. This can be observed regardless of the water depth and the configuration of the cable buoyancy section. This phenomenon needs to be considered for dynamic cable design.

Under the 180-degree configuration, due to the influence of the direction of platform movement, the cable is mainly affected by tension. As the result, the dynamic cable is stretched and the cable S-shaped curve may be broken, which causes the disappearance of the buffer effect, hence the tension value will be exceeded. This phenomenon is obvious under the configuration of shallow water with less dynamic cable movement space. In addition, when the mooring system generates a large restoring force, the excessive compression and curvature occur in the sag bend section of the dynamic cable. But this phenomenon is improved in cases 2 and 3. In conclusion, under the 180-degree configuration of the cable, whether the S-curve of the cable can be maintained and the bending of the dynamic cable should be considered.

In conclusion, based on the simulation results of dynamic cables, it is easier to design dynamic cables in deeper water (100 meters). As the water depth increases, rooms for tension and compression of dynamic cables also increases, and it is more appropriate with material limitations in terms of tension and curvature. Designing of the dynamic cable in shallow water areas (50 meters) is more difficult, because the movement space of the cable is limited by the depth of the water. Even if the deep buoyancy section and double buoyancy module are used, it is still difficult to meet the constraints of tension and curvature. Only the 0-degree cable configuration of cases 2 and 3 can meet the material constraints of the cable.

REFERENCES

Alexandre, A., Percher, Y., Choisnet, T., Buils Urbano, R., & Harries, R. (2018, November). Coupled analysis and numerical model verification for the 2MW Floatgen demonstrator project with IDEOL platform. In *International Conference on Offshore Mechanics and Arctic Engineering* (Vol. 51975, p. V001T01A032). American Society of Mechanical Engineers. https://doi.org/10.1115/IOWTC2018-1071

Chao, W. T., Young, C. C. (2006). Extreme value analysis for extreme atmospheric conditions in taiwan offshore wind farm. *Proceedings of the 28th Ocean Engineering Conference in Taiwan, 28*, 688-695. http://www.tsoe.org.tw/downloads/thesis/2020E112.pdf (In Chinese)

Chuang, T. C., Yang, W. H., & Yang, R. Y. (2021). Experimental and numerical study of a barge-type FOWT platform under wind and wave load. *Ocean Engineering, 230,* 109015. https://doi.org/10.1016/j.oceaneng.2021.109015

Demonstration Incentives for Offshore Wind Power 2019. https://law.moj.gov.tw/LawClass/LawAll.aspx?pcode=J0130063 (In Chinese)

Lai, Z. N. (2018). *Electrical and mechanical configuration planning of offshore substation*. Taiwan Power Company. https://report.nat.gov.tw/ReportFront/PageSystem/reportFileDownload/C10604313/002 (In Chinese)

Rentschler, M. U., Adam, F., & Chainho, P. (2019). Design optimization of dynamic inter-array cable systems for floating offshore wind turbines. *Renewable and Sustainable Energy Reviews*, *111*, 622-635. https://doi.org/10.1016/j.rser.2019.05.024

Rentschler, M. U., Adam, F., Chainho, P., Krügel, K., & Vicente, P.C. (2020). Parametric study of dynamic inter-array cable systems for floating offshore wind turbines. *Marine Systems & Ocean Technology*, *15* (1), 16-25. https://doi.org/10.1007/s40868-020-00071-7

Shelley, S. A., Boo, S. Y., Kim, D., & Luyties, W. H. (2020). Concept Design of Floating Substation for a 200 MW Wind Farm for the Northeast US. In Offshore Technology Conference. *Offshore Technology Conference*. https://doi.org/10.4043/30543-MS

Zhao, S., Cheng, Y., Chen, P., Nie, Y., & Fan, K. (2021). A comparison of two dynamic power cable configurations for a floating offshore wind turbine in shallow water. *AIP Advances*, *11* (3), 035302. https://doi.org/10.1063/5.0039221